Applied Thermal Engineering 148 (2019) 229–237

Contents lists available at ScienceDirect

Applied Thermal Engineering

journal homepage: www.elsevier.com/locate/apthermeng

Research Paper

Analytical modeling and optimization of phase change thermal management of a Li-ion battery pack

Mohammad Parhizi, Ankur Jain*

Mechanical and Aerospace Engineering Department, University of Texas at Arlington, Arlington, TX, USA

HIGHLIGHTS

- Carries out iterative heat transfer analysis of phase change cooling of Li-ion cells.
- Identifies key design trade-off between discharge rate and energy storage density.
- Compares the performance of phase change cooling with convective cooling.
- Contributes towards safe and efficient energy storage through effective cooling.

ARTICLE INFO

Keywords:
Lithium ion battery
Battery safety
Thermal management
Phase change cooling
Thermal runaway

ABSTRACT

Thermal management of Li-ion cells is critical for safety and performance of energy conversion and storage in battery packs in a variety of applications. Phase change cooling is a promising approach towards this goal. In contrast with several recent papers on experimental measurements of this approach, there is a distinct lack of literature in theoretical modeling of phase change cooling of Li-ion cells. This paper presents a theoretical model for solving the coupled heat transfer problem involving the cooling of a heat-generating Li-ion cell with a phase change material. Results show that while phase change cooling effectively reduces cell surface temperature, the cell core continues to remain quite hot. Improvement in cell thermal conductivity is shown to be critical for fully benefiting from phase change cooling. On the other hand, the impact of increasing thermal conductivity of the phase change material plateaus out at large values. Trade-offs between thermal management and energy storage density of a Li-ion battery pack are analyzed by quantifying the extent of temperature rise and reduction in energy storage density at large discharge rates. Comparison of phase change cooling with convective cooling is also presented, indicating key trade-offs in these approaches. These results contribute towards understanding the fundamentals of phase change cooling of Li-ion cells, as well as improving the performance of practical thermal management systems for Li-ion cells.

1. Introduction

Li-ion cells are used commonly for energy storage and conversion in a variety of applications including electric vehicles, renewable energy storage, consumer electronics, etc. [1,2]. Despite favorable electrochemical characteristics compared to competing technologies, Li-ion cells often suffer from overheating due to excessive heat generation [3,4], which has severely limited the application of this technology. Overheating is undesirable for both safety and performance. For example, current draw from a cell is often throttled in order to limit temperature rise, which reduces cell performance and lowers the power density of the battery pack. Excessive temperature rise in a Li-ion cell may also result in thermal runaway [5–8], which causes severe safety problems due to fire and explosion. Some fundamental reasons behind these severe thermal challenges in a Li-ion cell include poor thermal conductivity within the cell [9,10], non-linear temperature-dependent heat generation [7,8], particularly at high temperatures, and the stacking of cells very close to each other in a battery pack in order to maximize energy storage density [11].

Due to the reasons outlined above, thermal management of a Li-ion battery pack is of utmost importance, particularly for aggressive applications that require large discharge rates. For reference, discharge rate of a cell is often represented by its C-rate [3,4], which is the reciprocal of the time needed for complete discharge in hours. The larger the C-rate, the more aggressive is the discharge process in terms of heat generation rate [3,4]. A number of thermal management approaches

* Corresponding author at: 500 W First St, Rm 211, Arlington, TX 76019, USA.
E-mail address: jaina@uta.edu (A. Jain).

https://doi.org/10.1016/j.applthermaleng.2018.11.017
Received 25 June 2018; Received in revised form 2 November 2018; Accepted 5 November 2018
Available online 07 November 2018
1359-4311/

have been investigated in the past, and are well summarized in multiple review papers [3]. These include cold plate cooling [12,13], single phase convective cooling [14,15], heat pipe cooling [16,17], etc. Innovations in materials within the cell have been pursued in order to improve thermal conduction within the cell [18]. Both water and air have been used as coolants in battery packs [11,15]. A variety of heat pipe configurations including oscillating heat pipes have been implemented, both within a single cell and between cells in a battery pack [16,17]. The thermal effect of Boron Nitride coating on the cell casing has been investigated [19].

In contrast to thermal management approaches outlined above, phase change cooling involving melting and solidification may offer many advantages. A much greater heat removal rate may be achieved through phase change cooling compared to single phase thermal management due to the large latent heat associated with phase change. Due to its promising nature, experimental investigation of phase change cooling of Li-ion cells has been reported in several recent papers [20–24]. Experimental measurements of the performance of phase change materials (PCMs) such as paraffin wax for cooling of Li-ion cells have been carried out, and a significant reduction in cell temperature has been reported [21,25]. A number of innovative materials and composites, such as metal foams have been investigated for further improving the performance of phase change cooling through thermal conductivity enhancement [20,21,24,25]. Experiments have shown that phase change cooling can prevent propagation of thermal runaway induced by nail penetration to neighboring cells [22]. However, phase change cooling may lead to increased system complexity. Particularly, in the context of a Li-ion battery pack, the insertion of phase change material between cells reduces energy storage density. As a result, there is a need for careful co-optimization of PCM cooling with other system-level performance characteristics, for which, theoretical modeling is critical.

In comparison with the extensive literature available on measurements of phase change thermal management in Li-ion cells, there is a lack of work on theoretical modeling of these processes. Rigorous theoretical modeling is critical not only for fully optimizing the benefits of phase change cooling, but also for balancing trade-offs that exist with other system-level performance parameters such as energy storage density. Some simulation models using commercial finite-element tools are available [21,26], but these do not provide good analytical insight into the fundamental nature of the problem. Rigorous theoretical analysis of this problem is complicated considerably by the non-linear nature of phase change [27], making it difficult to analyze using standard theoretical tools. The coupling between phase change heat transfer and thermal conduction within the cell as well as electrochemical heat generation further complicates this problem. From a heat transfer perspective, this is a coupled problem [28–30], involving thermal conduction in a heat-generating body and phase change heat transfer in the coolant. While these two modes of heat transfer have been individually analyzed extensively, the coupled problem has not been paid much attention. For example, while the well-known Stefan problem addresses phase change in an infinite body with a constant temperature boundary condition [27], the presence of thermal conduction in a heat-generating solid body – the Li-ion cell in this case – makes the problem much more difficult to solve.

A good theoretical understanding of this problem is important for many practical reasons. The inclusion of a phase change material in a battery pack reduces overall energy density, since the phase change material increases pack weight and volume without contributing to electrochemical energy storage. A robust theoretical model can help understand the minimum amount of phase change material needed for a given cell undergoing a specific discharge, and therefore avoid overdesign of thermal management. A robust theoretical model can also help predict the effect of PCM cooling on internal temperature of the cell, which is critical for cell performance and safety, but is difficult to measure directly. Predictions from a theoretical model can also be used for accurate thermal management design in conditions where experimental data may not be available in advance. A theoretical model also helps understand the parametric dependence of the thermal characteristics of the system on various parameters such as thermal properties of the cell and phase change material, geometry, dimensions, etc.

This paper presents a theoretical model for predicting the transient temperature distribution in the cooling of a heat-generating Li-ion cell with a phase change material. The novelty of the theoretical approach in this work lies in solving the energy conservation equations in the two bodies in an iterative fashion to determine the transient temperature fields in both. This approach offers significantly reduced computational time compared to finite element simulations, and provides key insights into the fundamental nature of PCM cooling of Li-ion cells. A key result from this work is that while improving thermal conductivity of the PCM reduces cell surface temperature through greater melting rate, it does not effectively cool the core of the cell, which remains a key shortcoming of PCM cooling. Most of the past experimental work evaluates the effectiveness of PCM cooling based on surface temperature measurement alone, whereas, this work shows that PCM cooling provides only limited benefit to the core temperature. Results show that improving thermal conductivity of the cell is critical for fully benefiting from PCM thermal management. Another key contribution of this work is the analysis of the system-level trade-off between thermal management effectiveness and energy storage density. This paper not only develops a good theoretical understanding of heat transfer during phase change thermal management of a Li-ion cell, but also contributes towards understanding key design trade-offs in practical thermal management systems for Li-ion cells.

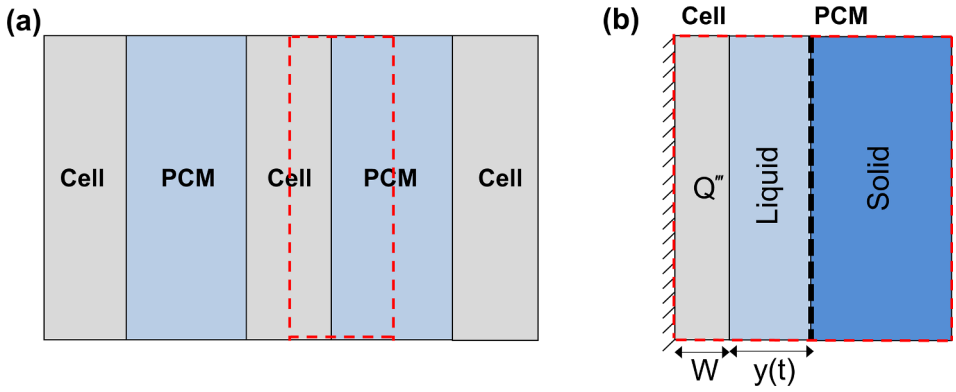

Fig. 1. (a) Schematic of a prismatic Li-ion battery pack with phase change cooling in the repeating unit is shown; (b) Schematic of the overall coupled heat transfer problem in the repeating unit.

2. Mathematical modeling

Fig. 1(a) shows a schematic of the geometry of a battery pack with multiple prismatic Li-ion cells being cooled by a phase change material inserted between cells. Assuming uniformly spaced cells in a single direction, symmetry could be used to analyze only one repeating unit of the pack, shown in Fig. 1(b). Within this region, the relevant heat transfer processes include heat generation inside the cell of half-thickness W, thermal conduction within the cell, heat transfer from the cell into the phase change material at the cell-PCM interface, conduction into the PCM and phase change at the liquid-solid interface. Thermal contact resistance between the cell and PCM is neglected due to the expected intimate contact between the cell surface and PCM that melts and solidifies repeatedly. Note that the location of the liquid–solid interface, $y(t)$, is a function of time – as more and more heat is absorbed by the PCM, $y(t)$ increases with time.

Given the complicated and coupled nature of this coupled heat transfer problem, a direct solution may not be possible. Instead, this problem is solved by splitting into two sub-problems, which are solved individually while ensuring continuity of temperature and heat flux at the cell-PCM interface. The two sub-problems are shown schematically in Fig. 2. The cell sub-problem involves a certain heat flux $q''(t)$ leaving the cell at the cell-PCM interface, while the PCM sub-problem involves a certain time-dependent temperature $T_0(t)$ at the interface. Both $q''(t)$ and $T_0(t)$ are unknown. However, this problem can be solved in an iterative process, wherein a certain $T_0(t)$ is guessed and used to solve the PCM sub-problem. Based on the solution of this problem, interfacial heat flux is calculated and used to solve the cell problem, which requires the heat flux as an input. The solution of the cell problem is then used to determine the interface temperature $T_0(t)$, which is used to improve the initial guess of the interfacial temperature. The process is then repeated iteratively until there is acceptably small change in $T_0(t)$ from one iteration to the next. Fig. 3 shows a flowchart of the iterative method for determining the solution of the coupled heat transfer problem.

Such an iterative process has been used for solving a variety of coupled problems [11,29], including the problem of single phase cooling of cells in a Li-ion battery pack. The novelty of the approach adopted in this paper lies in the coupled analysis of the much more complicated phase change problem. Further, unlike past papers, where only steady state problems were solved [11,29], this paper addresses a more realistic, transient problem, involving increasing cell temperature with time, as well as a phase change front in the PCM that advances with time.

The iterative approach described above requires analytical solutions for the cell and PCM sub-problems, given the interfacial heat flux and temperature respectively as functions of time. These solutions are derived in the next two sub-sections.

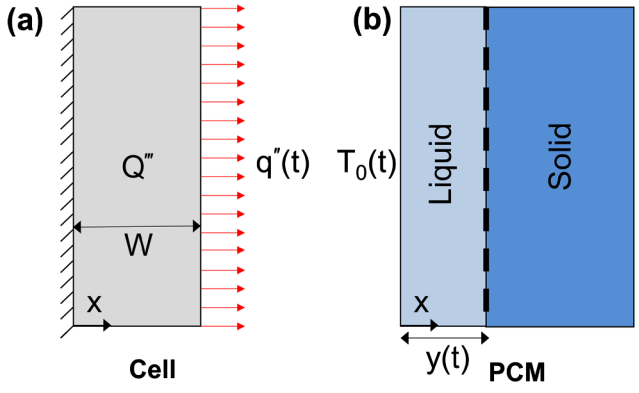

Fig. 2. Schematic of the two heat transfer sub-problems: (a) Cell problem; (b) PCM problem.

2.1. Solution for the PCM sub-problem

The PCM sub-problem involves a one-dimensional phase change material of thermal conductivity k_p, specific heat capacity $C_{p,p}$, latent heat L and mass density ρ_p being heated up by an imposed temperature $T_0(t)$ at the boundary $x = 0$, as shown in Fig. 2(b). Due to this temperature boundary condition, the PCM slowly melts, starting at $x = 0$. The liquid-solid interface, located at $x = y(t)$ progresses towards the right as time passes, and more and more liquid is formed due to phase change. Convection in the recently formed liquid phase is neglected. This is a generalization of the well-known Stefan problem, in which a constant temperature boundary condition is imposed, as opposed to a time dependent $T_0(t)$ considered here. The governing energy conservation equation for $T_p(x,t)$, the temperature field in the melted PCM is

$$\frac{\partial^2 T_p}{\partial x^2} = \frac{1}{\alpha_p}\frac{\partial T_p}{\partial t} \quad 0 \leqslant x \leqslant y(t) \tag{1}$$

along with the following boundary condition

$$T_p = T_0(t) \quad \text{at } x = 0 \tag{2}$$

where $T_0(t)$ is the imposed time-dependent temperature boundary condition on the face of the PCM.

In addition, energy conservation and continuity of temperature at liquid-solid front requires that

$$T_p = T_m \quad \text{at } x = y(t) \tag{3}$$

and

$$-k_p\left[\frac{\partial T_p}{\partial x}\right]_{x=y(t)} = \rho_p L\frac{dy}{dt} \quad \text{at } x = y(t) \tag{4}$$

where T_m is the PCM melting temperature. Eqs. (1) through (4) represent a non-linear phase change problem, which is further complicated by the time-dependence in the boundary condition at $x = 0$. While a direct analytical solution for this general problem is likely not possible, several approximate analytical methods have been presented in the literature for solving similar problems, including integral methods [31], perturbation methods [30], etc. In this case, the perturbation method [30] is used. Briefly, the solution is assumed to be a power series expansion based on the Stefan number, $Ste = \frac{C_{p,p}(T_m - T_{ref})}{L}$ where T_{ref} is a reference temperature [27,30]. The problem is transformed in order to change one of the dependent variables from t to the interface location $y(t)$. The power series form of the temperature solution is inserted into the governing equation and simplified using boundary conditions. Through a term-by-term comparison, a solution for the temperature profile in the liquid is derived in terms of the interface location. Finally, the location of the phase change front itself is determined by using the principle of energy conservation at the phase change front [30], given by Eq. (4). The interface heat flux is then determined by differentiating the liquid temperature distribution as follows:

$$q''_{PCM}(t) = -k(T_m - T_{ref})\left[-\frac{f(t)}{y(t)} - Ste\frac{f(t)\left(f(t) + 2\frac{f'(t)}{y'(t)}y(t)\right)}{6y(t)} + Ste^2\frac{f(t)\left(40\left(\frac{f'(t)}{y'(t)}\right)^2 y^2(t) + 85f(t)\frac{f'(t)}{y'(t)}y(t) + 19f^2(t) + 8\frac{f''(t)}{y'^2(t)}f(t)y^2(t)\right)}{360y(t)}\right] \tag{5}$$

where $f(t)$ is the non-dimensional time-dependent boundary temperature given by [30]

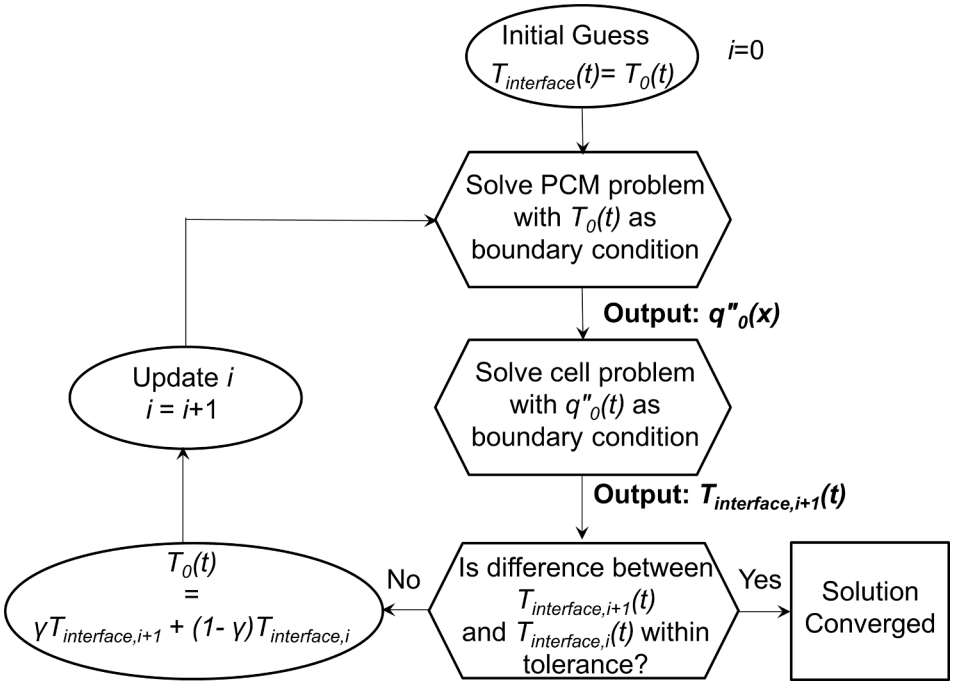

Fig. 3. Flowchart of the iterative process for determining the solution of the coupled heat transfer problem.

$$f(t) = \frac{T_0(t) - T_m}{T_m - T_{ref}} \tag{6}$$

and the liquid-solid interface location, $y(t)$ is given by [30]

$$y(t) = \left[2\alpha_p (Ste) \int_0^t f(\tau) \left(1 - \frac{Ste}{3} f(\tau) + \frac{7Ste^2}{45} f(\tau)^2 \right) d\tau \right]^{\frac{1}{2}} \tag{7}$$

where α_p is the PCM thermal diffusivity. The interfacial heat flux determined in this manner from Eq. (5) can be used to solve the cell sub-problem as described below.

2.2. Solution for the cell sub-problem

The cell sub-problem involves a one-dimensional body of thickness W, thermal conductivity k_c, specific heat capacity $C_{p,c}$ and thermal diffusivity α_c generating heat at a volumetric rate of Q''', as shown in Fig. 2(a). There is zero heat flux at $x = 0$ due to symmetry, whereas a certain outgoing heat flux $q''(t)$ is imposed on the boundary at $x = W$. The governing energy conservation equation for the temperature distribution in the cell, $T_c(x,t)$ is

$$\frac{\partial^2 T_c}{\partial x^2} + \frac{Q'''}{k_c} = \frac{1}{\alpha_c} \frac{\partial T_c}{\partial t} \tag{8}$$

Boundary conditions associated with Eq. (8) are

$$\frac{\partial T_c}{\partial x} = 0 \quad \text{at } x = 0 \tag{9}$$

and

$$-k_c \frac{\partial T_c}{\partial x} = q''(t) \quad \text{at } x = W \tag{10}$$

Due to the two non-homogeneities in the problem, the solution is split into two parts, each of which account for one of the non-homogeneities. Since heat generation is assumed to be constant and spatially uniform, the solution for the heat generation part is quite straightforward as follows:

$$T_{c1}(t) = \frac{Q'''}{\rho_p C_{p,c}} t \tag{11}$$

The method of undetermined parameters [32,33] is used for deriving the second part of the solution that accounts for the time-dependent heat flux. The solution is assumed to be a series sum of eigenfunctions of the corresponding homogeneous problem.

$$T_{c2}(x, t) = \sum_{n=0}^{\infty} C_n(t) \text{Cos}(\lambda_n x) \tag{12}$$

where $\lambda_n = \frac{n\pi}{W}$ are the eigenvalues of the corresponding homogenous problem. The unknown coefficients $C_n(t)$ in Eq. (12) are determined by differentiating Eq. (12) with respect to time, substituting in the governing energy equation and using the boundary conditions and the principle of orthogonality to simplify. This results in an ordinary differential equation for $C_n(t)$

$$C_n' + \alpha_c \lambda_n^2 C_n = \frac{\alpha_c}{N} \left(\frac{-q''(t)}{k_c} \right) \text{Cos}\lambda_n W \tag{13}$$

for which, the solution, assuming zero temperature rise at $t = 0$ is

$$C_0 = -\frac{\alpha_c}{k_c W} \int_0^t q''(\tau) d\tau \tag{14}$$

$$C_n = -\frac{2\alpha}{k_c W} Cos(\lambda_n W) \int_0^t q''(\tau) \exp(-\alpha_c \lambda_n^2 (t - \tau)) d\tau \tag{15}$$

where N_n is the eigenvalue norm and $n = 1, 2, 3...$

This completes the solution of the cell sub-problem shown in Fig. 2(a), from where the interface temperature is found to be

$$\begin{aligned} T_{\text{int erface}}(t) = T_c(x = W, t) = & -\frac{\alpha_c}{k_c W} \int_0^t q''(\tau) d\tau \\ & + \sum_{n=1}^{\infty} -\frac{2\alpha_c}{k_c W} \text{Cos}^2(\lambda_n W) \int_0^t q''(\tau) \exp(-\alpha_c \lambda_n^2 (t - \tau)) d\tau \\ & + \frac{Q'''}{\rho_c C_{p,c}} t \end{aligned} \tag{16}$$

Note that in this case, the internal heat generation rate Q''' heats up the cell whereas the heat flux $q''(t)$ may cool the cell down. Therefore, for this sub-problem, the cell temperature may go up or down with time depending on the relative magnitudes of Q''' and $q''(t)$.

2.3. Iterative process

The iterative procedure for solving the coupled problem starts with guessing an initial cell-PCM interface temperature curve, $T_0(t)$. The PCM sub-problem is then solved using $T_0(t)$ as the boundary condition as discussed in Section 2.1. The solution provides the cell-PCM interface heat flux, $q''(t)$ which can be used to solve the cell sub-problem. Solution to the cell sub-problem provides a new interface temperature $T_0(t)_{new}$, which is used to repeat the iterative procedure. The interface heat flux leaving the cell, $q''(t)$, may be large in the first few iterations due to the large temperature gradient between the cell and PCM caused by the initial interface temperature. This large outgoing heat flux may result in negative temperature, particularly if the initial interface temperature is not accurate. To avoid such problems, the interface temperature curve is blended with that from the previous iteration using a low value of the blending factor in order to prevent instability in the iterative process. Fig. 3 shows a flowchart of the iterative method, including the blending process.

In summary, the iterative theoretical model presented in this section predicts temperature distribution in the cell and the surrounding PCM, taking into account various heat generation and heat transfer processes, including propagation of the phase change front. The next section discusses the validation of and various results obtained based on this theoretical model.

3. Results and discussion

3.1. Validation and optimization of analytical model

Since the analytical solution approach is iterative in nature, it is important to track the predicted temperature distribution over multiple iterations. A realistic case is considered, wherein a 20 mm thick cell generating heat at 87,000 Wm^{-3} corresponding to a C-rate of 5C [34] is being cooled by paraffin wax, a commonly used phase change material of thermal conductivity $k_p = 0.2\,W/m^{-1}K^{-1}$ and latent heat $L = 270.7\,kJ\,kg^{-1}$ [25].

In these conditions, the computed temperature at the cell-PCM interface is plotted as a function of time for multiple number of iterations in Fig. 4. The initial guess for the interface temperature as a function of time is also plotted. Fig. 4 shows that the temperature distribution changes rapidly in the first few iterations, but eventually stabilizes as it converges. Beyond seven iterations, there is minimal change in the temperature distribution from one iteration to the next. This shows that for the conditions assumed here, around seven iterations are sufficient

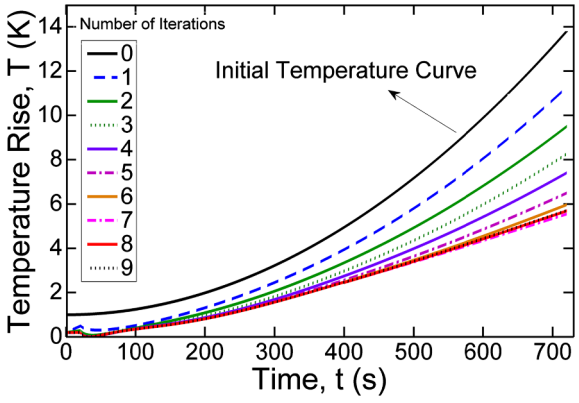

Fig. 4. Cell-PCM interfacial temperature rise, $T_0(t)$ as a function of time for multiple number of iterations, including the initial temperature curve. Values for PCM thermal conductivity and latent heat are $k_p = 0.2\,Wm^{-1}K^{-1}$ and $L = 270.7\,kJ\,kg^{-1}$ respectively. The cell generates heat at 87,000 Wm^{-3}, corresponding to 5C discharge rate. Plot indicates that the temperature distribution converges within around seven iterations.

for obtaining the analytical solution. This is an important insight in optimizing the computation of the analytical model since each iteration requires additional computation time. Additional computations have been carried out with multiple other initial guesses to verify that the temperature field converges to the same value regardless of the initial guess. Note that these results are obtained with a blend factor $\gamma = 0.1$. The convergence could possibly be obtained faster with a larger value of γ. However, in case the initially assumed temperature distribution deviates significantly from the correct temperature distribution, a large value of γ may lead to instability. As a result, a conservative value of $\gamma = 0.1$ is used throughout this work.

Analytical solutions for the two sub-problems discussed in Sections 2.1 and 2.2 are also validated by comparison of the predicted temperature distribution for specific cases with finite-element simulation results for a set of parameters representative of realistic conditions. In order to validate the PCM model, a one-dimensional transient finite-element simulation is carried out in ANSYS CFX. A phase change material of thermal conductivity $k_p = 0.2\,Wm^{-1}K^{-1}$ and latent heat $L = 270.7\,kJkg^{-1}$ is considered. A time-dependent temperature boundary condition $T_0(t) = 20 + \frac{t}{100}$is imposed on the material at $x = 0$ for 1000 s. Note that T_0 is expressed relative to T_m. To carry out the phase change simulation, the same geometry as Fig. 2(b) is modeled in ANSYS CFX. A mesh sensitivity study shows that 2500 nodes are sufficient for grid independence. PCM is defined as a homogenous binary mixture of liquid and solid where the liquid part has the specific reference enthalpy of $270.7\,kJkg^{-1}$. Saturation properties for the binary mixture are defined as well based on the PCM properties. The analytical model is used for computing the melting front $y(t)$ and compared against finite-element simulation results. As shown in Fig. 5(a), the two are in good agreement with each other. While the analytical model can be computed quite rapidly, within 60 s, the transient finite-element simulation takes about 20 min, even when not accounting for the time needed for setup and grid generation prior to the finite element computations.

Similar to the PCM sub-problem, the cell sub-problem discussed in Section 2.2 is also validated by comparison against finite-element simulations. For a cell of thermal conductivity $k_c = 0.2\ Wm^{-1}K^{-1}$ and generating 10^6 Wm^{-3} with a given heat flux $q''(t)$ on its boundary at $x = W$, the predicted interface temperature as a function of time and compared against finite element simulation results in Fig. 5(b). The interfacial heat flux as a function of time, $q''(t)$ assumed for this comparison is also shown in Fig. 5(b). In this case, the interfacial temperature initially decreases due to the increase in heat flux leaving the cell and insufficient generated heat reaching the boundary. As time progresses, however, more and more heat generated in the cell diffuses to the boundary, and also, heat flux imposed on the boundary decreases, resulting in an increase in the cell surface temperature. Throughout the entire period, the predicted interface temperature is in good agreement with finite-element simulation results. In this case, 500 eigenvalues are considered for the analytical solution represented by Eq. (16). It is verified that additional eigenvalues do not significantly change the predicted temperature distribution.

Comparison of the analytical models against finite-element simulations shown in Fig. 5 provides a validation of these models. Phase change based thermal management of Li-ion cells in a variety of scenarios is analyzed next.

3.2. Effect of phase change material properties

Thermal properties of the phase change material are likely to be important for the design of phase change based thermal management because this process is driven primarily by heat absorption during phase change and because heat entering the phase change material must first conduct through the melted liquid before being absorbed in the phase change process. While phase change materials have reasonably high latent heat, the thermal conductivity is usually low, and

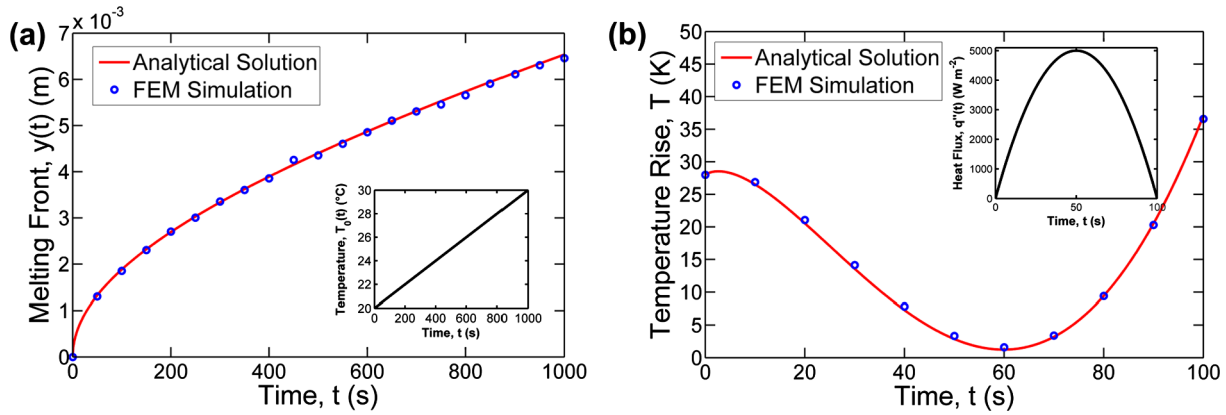

Fig. 5. Comparison of the analytical solution (red curves) and a finite element simulation carried out in ANSYS-CFX (blue circles) for the two sub-problems: (a) PCM melting front, $y(t)$ as a function of time for a time-dependent temperature boundary condition $T_0(t) = 20 + \frac{t}{100}$. (b) Cell core temperature rise as a function of time for a given heat flux $q''(t)$ on the $x = W$ boundary. Plots indicate good agreement between analytical method and finite-element simulations throughout the entire period. PCM thermal conductivity and latent heat are taken to be $k_p = 0.2\ \mathrm{Wm^{-1}K^{-1}}$ and $\mathrm{L} = 270.7\ \mathrm{kJ\,kg^{-1}}$ respectively, corresponding to paraffin wax. Cell thermal conductivity and internal heat generation are taken to be $k_c = 0.2\ \mathrm{Wm^{-1}K^{-1}}$ and $Q''' = 10^6\ \mathrm{Wm^{-3}}$ respectively.

multiple papers have attempted to improve thermal conductivity through various mechanisms such as insertion of metal foams, fillers, etc. [20–25]. The expected impact of these thermal property enhancements on cooling effectiveness is investigated here.

For a cell with a thermal conductivity of $k_c = 0.2\ \mathrm{Wm^{-1}K^{-1}}$ – a realistic value based on past measurements [9] – undergoing 10C discharge, peak temperature rise in the cell that occurs at its core is plotted in Fig. 6(a) as a function of time for multiple values of the phase change material thermal conductivity, assuming the latent heat to be $270.7\ \mathrm{kJ\,kg^{-1}}$. Fig. 6(b) shows the corresponding cell surface temperature rise as a function of time. These plots show that while improving PCM thermal conductivity has a significant impact on the cell surface temperature rise, there is only a minor impact on cell core temperature rise. This happens because while a greater PCM thermal conductivity ensures better heat transfer through the PCM, and therefore, reduced cell surface temperature, the core temperature remains relatively unaffected due to the slower rate of thermal conduction within the cell. The impact of improving PCM thermal conductivity on the core temperature of the cell saturates once the thermal conductivity reaches a threshold. Beyond that, there is minimal impact of further improving PCM thermal conductivity on the cell core temperature because the cell thermal conductivity is the rate-limiting property. This is a critical issue for safety of Li-ion cells and highlights a key limitation of attempts to improve thermal conductivity of phase change materials.

Fig. 7 presents a similar investigation of the effect of latent heat of the phase change material. In this case, thermal conductivity is held constant at $k_p = 0.2\ \mathrm{Wm^{-1}K^{-1}}$. Fig. 7(a) and (b) plot temperature rise at the cell core and surface respectively for multiple values of the latent heat at 6C discharge rate. Similar to thermal conductivity, a strong impact of latent heat on the cell surface temperature is seen. However, similar to Fig. 6(a), the core temperature does not reduce significantly with increasing value of the latent heat, once again due to the throttling effect of the relatively poor thermal conductivity of the cell itself.

These results indicate that improving PCM thermal properties alone, as has been proposed in several recent papers [20–25], does not ensure effective cooling throughout the cell. Fundamentally, this occurs because, even if the PCM itself may have excellent thermal properties, low thermal conductivity of the Li-ion cell severely limits the rate of heat transfer from within the cell into the PCM. Therefore, enhancing heat transfer within the cell and understanding the impact of improvements in cell thermal conductivity is equally important, and is investigated next.

3.3. Effect of cell properties

Measurements reported in the past show that Li-ion cells have relatively poor thermal conductivity, around 0.1–1.0 $\mathrm{Wm^{-1}K^{-1}}$ [3,9,35], due to which thermal conductivity may be a dominant parameter in determining the effectiveness of phase change thermal management. In order to investigate this, temperature distributions in the cell and phase change material are computed for a discharge rate of 6C. Fig. 8(a) plots these temperature distributions at the end of the

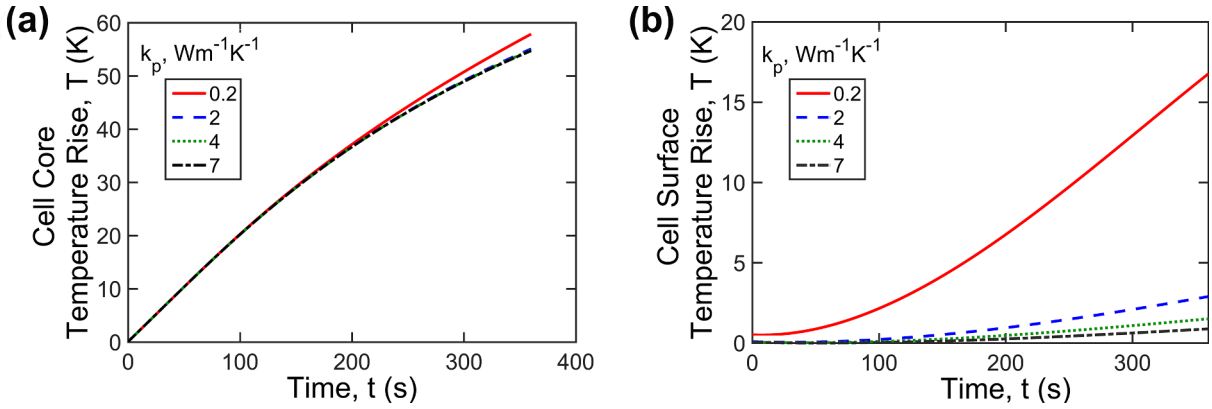

Fig. 6. Effect of PCM thermal conductivity on (a) Cell peak temperature rise as a function of time; and (b) Cell surface temperature rise as a function of time. Results indicate that improving PCM thermal conductivity significantly improves cell surface temperature but not the cell core temperature.

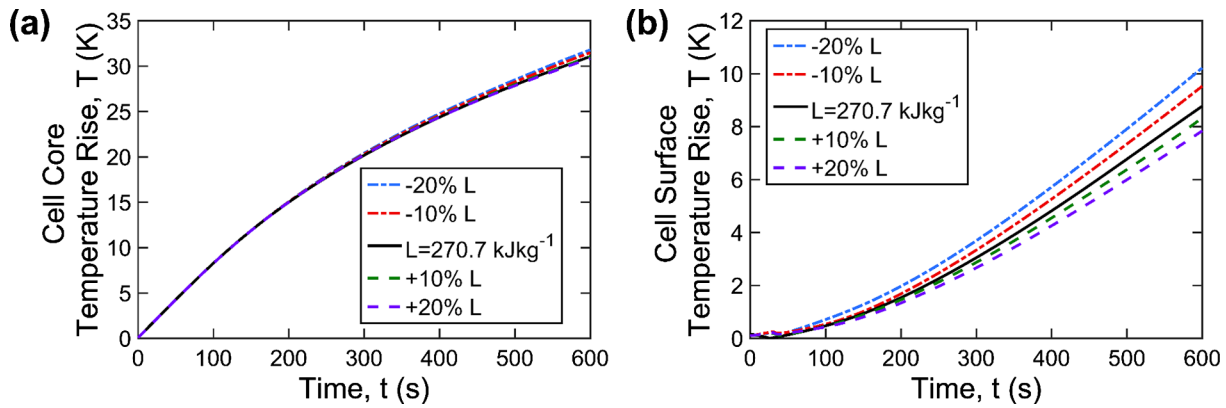

Fig. 7. Effect of PCM latent heat on (a) Cell core temperature rise as a function of time; and (b) Cell surface temperature rise as a function of time. Results indicate that improving latent heat improves cell surface temperature but not the cell core temperature.

discharge process for different values of the cell thermal conductivity while holding all other parameters constant. A phase change material of thermal conductivity $k_p = 0.2$ $\mathrm{Wm^{-1}K^{-1}}$ and latent heat $L = 270.7\,\mathrm{kJ\,kg^{-1}}$ [25] is assumed. Fig. 8(a) shows significant improvement in cell temperature distribution at higher values of cell thermal conductivity, including at the core of the cell. Up to 50% reduction in cell core temperature is seen for cell thermal conductivity of 2.0 $\mathrm{Wm^{-1}K^{-1}}$ compared to the baseline value of 0.2 $\mathrm{Wm^{-1}K^{-1}}$, unlike the case of improved PCM thermal conductivity, which reduces surface temperature significantly but not the core temperature. In addition, Fig. 8(a) also shows significant improvement in temperature uniformity across the cell, which is an important consideration in electrochemical performance of the cell.

The importance of cell thermal conductivity has been largely overlooked in past work on PCM thermal management, which has focused mostly on thermal properties of the PCM. Further, note that improving thermal conductivity of a Li-ion cell remains a key challenge due to the complicated, heterogeneous nature of the cell, with only limited work available, based on material and interfacial changes within the cell [18].

For the same conditions, Fig. 8(b) plots the solid-liquid interface position $y(t)$, measured from the cell-PCM interface as a function of time. This plot shows higher rate of phase change in the PCM with increasing cell thermal conductivity. This directly results from improved heat diffusion through the cell, leading to greater heat absorption by the PCM. Fig. 8(b) further confirms that increasing cell thermal conductivity is critical for fully benefitting from phase change based thermal management.

3.4. Trade-off between thermal management and energy storage density

Heat generation rate in a Li-ion cell can change significantly with time due to changes in the external load and discharge current. In general, the greater the discharge current, the higher is the heat generation rate. Any passive thermal management strategy, such as one based on phase change materials, must take these dynamics into account and be able to effectively cool the worst-case discharge rate expected during the duty cycle of the battery pack. As the discharge rate goes up, the volumetric heat generation rate also goes up, but the duration of heat generation reduces because the cell discharges faster [34]. In order to understand the effect of these parameters on thermal management, the peak temperature in the cell, which occurs at the cell core, is plotted in Fig. 9 as a function of time for a number of discharge rates. For these simulations, a phase change material of thermal conductivity of 0.2 $\mathrm{Wm^{-1}K^{-1}}$ and latent heat of 270.7 $\mathrm{kJ\,kg^{-1}}$ is assumed. Values for heat generation rate and thermal conductivity are taken from past measurements [9,34]. Fig. 9 shows that the effect of increased heat generation rate at larger C-rates dominates over the effect of reduced time period, due to which the peak temperature is significantly greater at higher C-rates. To investigate this further, Fig. 10 plots the maximum cell temperature, which occurs at the end of the discharge period as a function of C-rate. As expected, the peak temperature increases as discharge rates increases. Further, as the discharge rate goes up, the phase change front also increases, indicating the need for more and more phase change material between cells in order to sustain phase change cooling throughout the discharge process. Note that the phase change material in the battery pack is electrochemically passive, and therefore reduces energy storage density – a key performance

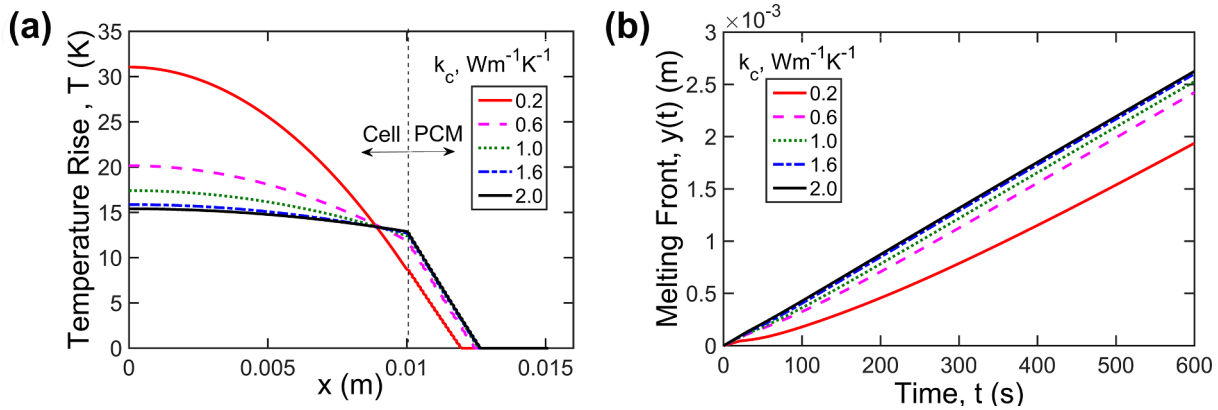

Fig. 8. Effect of cell thermal conductivity on (a) Cell peak temperature rise; and (b) PCM melting front, $y(t)$ as a function of time. Plots indicate significant improvement in cell core temperature and higher rate of phase change in the PCM with increasing cell thermal conductivity. PCM thermal conductivity and latent heat are taken to be $k_p = 0.2$ $\mathrm{Wm^{-1}K^{-1}}$ and $L = 270.7\,\mathrm{kJ\,kg^{-1}}$ respectively, corresponding to paraffin wax.

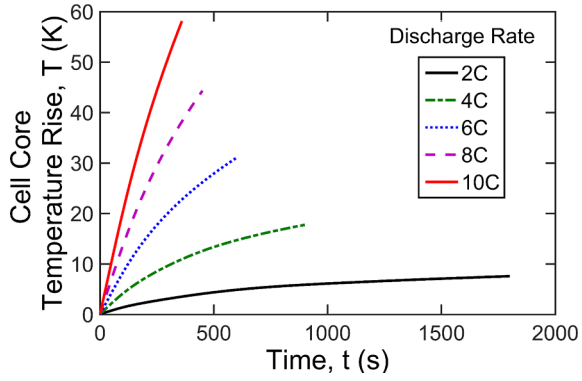

Fig. 9. Effect of cell discharge rate on the peak temperature rise as a function of time. Phase change material of thermal conductivity of 0.2 $Wm^{-1}K^{-1}$ and latent heat of 270.7 $kJ\,kg^{-1}$ is assumed. Heat generation values corresponding to different discharge rates are taken from past measurements [34]. Plot indicates that the effect of increased heat generation rate at larger C-rates overwhelms the reduced time period, due to which the peak temperature is greater at higher C-rates.

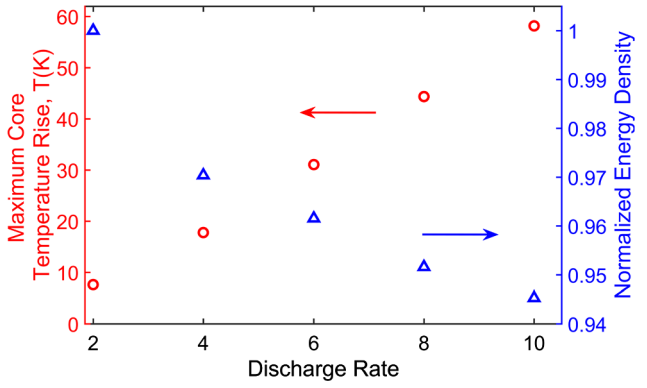

Fig. 10. Plot of the maximum cell core temperature rise and relative energy storage density of the battery pack as a function of C-rate. Plot indicates that at larger discharge rates, there is greater temperature rise, and hence more PCM needed for thermal management, resulting in reduced energy storage density of the battery pack.

parameter of the pack. To quantify this, Fig. 10 also plots the energy storage density of the battery pack on a relative scale accounting for the presence of the passive PCM in the pack. Fig. 10 shows that as the discharge rate goes up, the peak temperature rise goes up, and consequently, the energy storage density reduces due to need to include more and more PCM. This quantifies a fundamental, system-level trade-off in Li-ion battery pack design – large discharge rate inherently reduces energy storage density due to the need for greater thermal management. Many applications call for aggressive discharge rates, which Fig. 10 shows will result in greater temperature rise and reduced energy storage density. Based on overall system requirements, a balance between these performance parameters must be achieved.

3.5. Phase change vs forced convection thermal management

Finally, the phase change based thermal management approach is compared with traditional, single phase convective cooling of the battery pack. For this comparison, the same cell as shown schematically in Fig. 1(a) is considered, except with convective cooling with a heat transfer coefficient h instead of the phase change material. In this case, the transient temperature distribution in the cell can be easily derived to be [27]

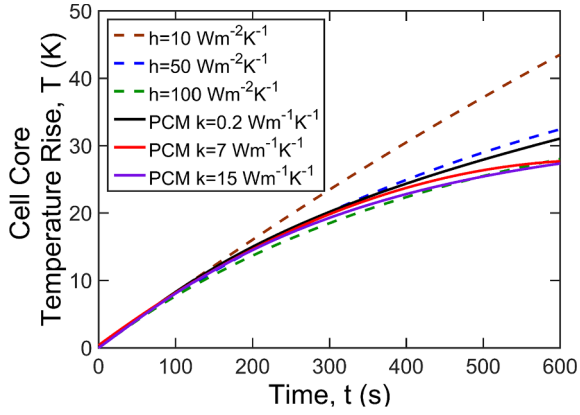

Fig. 11. Comparison of phase change cooling with convective cooling. Plot of peak temperature rise in the cell during 6C discharge rate as a function of time for multiple values of the convective heat transfer coefficient h. For comparison, plots for PCM cooling with baseline (k_p = 0.2 $Wm^{-1}K^{-1}$) and thermally enhanced (k_p = 7.0 $Wm^{-1}K^{-1}$ and 15.0 $Wm^{-1}K^{-1}$) cases are also plotted.

$$T(x,\,t) = \sum_{n=1}^{\infty}\left[\frac{\mathrm{Cos}(\lambda_n x)\exp(-\alpha\lambda_n^2 t)}{N(\lambda_n)}\int_{x'=0}^{W} -S(x')\mathrm{Cos}(\lambda_n x')dx'\right] \tag{17}$$

where

$$S(x) = -\frac{Q'''}{2k}(x^2 - W^2) + \frac{Q'''W}{h} \tag{18}$$

For the case of a 20 mm cell undergoing 6C discharge, Fig. 11 plots the peak temperature in the cell as a function of time for multiple values of the convective heat transfer coefficient h. For comparison, the peak temperature expected for phase change based cooling with a phase change material of k_p = 0.2 $Wm^{-1}K^{-1}$ and L = 270.7 $kJ\,kg^{-1}$ is also plotted as a function of time. Fig. 11 shows that convective cooling, even with fairly low heat transfer coefficient up to 50 $Wm^{-2}K^{-1}$ may be as effective as PCM-based thermal management assuming baseline PCM thermal conductivity. A higher convective heat transfer coefficient of 100 $Wm^{-2}K^{-1}$ compares well with the case of an improved PCM thermal conductivity of 7.0 $Wm^{-1}K^{-1}$ – a value that is at the higher end of the range reported in the literature [24]. This result is consistent with recent work where the performance of phase change cooling has been compared with forced convection cooling of Li-ion cells [36]. For comparison, Fig. 11 also plots the expected thermal response in case of a PCM with a very high thermal conductivity of 15 $Wm^{-1}K^{-1}$, and shows that the impact of improving thermal conductivity saturates – the curves for 7 $Wm^{-1}K^{-1}$ and 15 $Wm^{-1}K^{-1}$ are nearly identical. In this range, improving PCM thermal conductivity does not offer further improvement in performance.

This comparison demonstrates the limitations of PCM cooling in Li-ion cells because of the short time duration of heating. In many cases, convective cooling by itself may offer an attractive thermal management option. On the other hand, phase change thermal management is passive, easier to implement and does not require energy, whereas providing fluid flow and high convective heat transfer coefficient to the surface of each cell in a large battery pack complicates thermal management design, and may involve significant pressure drops, and therefore higher energy costs. Therefore, a holistic approach combining multiple thermal management may be more effective.

4. Conclusions

Phase change cooling of Li-ion cells is a promising approach for thermal management of battery packs, particularly due to its passive nature and minimal power requirement. Modeling of phase change cooling, such as one presented in this work, involves several theoretical

challenges. Insights gained from such analysis can be critical for optimization of thermal management systems, particularly when applied together with experimental data. For example, multiple papers have investigated thermal conductivity improvement of the phase change material for battery cooling. However, this work shows that while such an approach has a significant impact on the melting rate and the cell surface temperature, adequate cooling of the core of the cell requires substantial improvement in thermal conductivity of the cell. While this is consistent with the basic principles of heat transfer, it has not been recognized adequately in past work. The present theoretical model quantifies this key challenge in PCM based thermal management.

Results also highlight and quantify the key system-level trade-off between discharge rate and energy storage density, which can prevent needless overdesign of thermal management. Another important insight from this work is the comparison between phase change cooling and convective cooling. It is expected that the theoretical model and key results presented in this work will contribute towards accurate design of practical thermal management systems for Li-ion battery packs, eventually leading to improvement in safety and performance of energy conversion and storage devices.

The present theoretical approach ignores sensible heating of the PCM prior to phase change, which may occur if the melting temperature of the PCM is greater than ambient temperature. While this is unlikely to be a dominant effect due to the small value of Stefan number for most phase change materials, accounting for this may be an interesting direction for future work. Further, the model assumes perfect symmetry between cells in the battery pack, and needs to be extended to account for non-symmetric features in large battery packs. Further, integration of experiments with theoretical modeling is also an important direction for future work. Incorporation of the theoretical model presented here in practical Battery Management Systems (BMS) of large battery packs is also important. Finally, the impact of the phase change material in the battery pack on other battery functions, such as battery heating in a cold environment – relevant for automotive applications – is also important.

Acknowledgements

This material is based upon work supported by CAREER Award No. CBET-1554183 from the National Science Foundation.

References

[1] J.B. Goodenough, K.-S. Park, The Li-ion rechargeable battery: a perspective, J. Am. Chem. Soc. 135 (2013) 1167–1176.
[2] B. Scrosati, J. Garche, Lithium batteries: Status, prospects and future, J. Power Sources 195 (2010) 2419–2430.
[3] K. Shah, V. Vishwakarma, A. Jain, Measurement of multiscale thermal transport phenomena in Li-ion cells: a review, J. Electrochem. Energy Convers. Storage 13 (2016) 030801.
[4] T.M. Bandhauer, S. Garimella, T.F. Fuller, A critical review of thermal issues in lithium-ion batteries, J. Electrochem. Soc. 158 (2011).
[5] C.F. Lopez, J.A. Jeevarajan, P.P. Mukherjee, Characterization of lithium-ion battery thermal abuse behavior using experimental and computational analysis, J. Electrochem. Soc. 162 (2015).
[6] K. Shah, D. Chalise, A. Jain, Experimental and theoretical analysis of a method to predict thermal runaway in Li-ion cells, J. Power Sources 330 (2016) 167–174.
[7] M. Parhizi, M. Ahmed, A. Jain, Determination of the core temperature of a Li-ion cell during thermal runaway, J. Power Sources 370 (2017) 27–35.
[8] R. Spotnitz, J. Franklin, Abuse behavior of high-power, lithium-ion cells, J. Power Sources 113 (2003) 81–100.
[9] S. Drake, D. Wetz, J. Ostanek, S. Miller, J. Heinzel, A. Jain, Measurement of anisotropic thermophysical properties of cylindrical Li-ion cells, J. Power Sources 252 (2014) 298–304.
[10] K. Shah, S. Drake, D. Wetz, J. Ostanek, S. Miller, J. Heinzel, et al., Modeling of steady-state convective cooling of cylindrical Li-ion cells, J. Power Sources 258 (2014) 374–381.
[11] D. Chalise, K. Shah, R. Prasher, A. Jain, Conjugate heat transfer analysis of thermal management of a Li-Ion battery pack, J. Electrochem. Energy Convers. Storage 15 (2017) 011008.
[12] Y. Huo, Z. Rao, X. Liu, J. Zhao, Investigation of power battery thermal management by using mini-channel cold plate, Energy Convers. Manage. 89 (2015) 387–395.
[13] L. Jin, P. Lee, X. Kong, Y. Fan, S. Chou, Ultra-thin minichannel LCP for EV battery thermal management, Appl. Energy 113 (2014) 1786–1794.
[14] X. Xu, R. He, Research on the heat dissipation performance of battery pack based on forced air cooling, J. Power Sources 240 (2013) 33–41.
[15] M.R. Giuliano, A.K. Prasad, S.G. Advani, Experimental study of an air-cooled thermal management system for high capacity lithium–titanate batteries, J. Power Sources 216 (2012) 345–352.
[16] D. Anthony, D. Wong, D. Wetz, A. Jain, Improved thermal performance of a Li-ion cell through heat pipe insertion, J. Electrochem. Soc. 164 (2017).
[17] Q. Wang, B. Jiang, Q. Xue, H. Sun, B. Li, H. Zou, et al., Experimental investigation on EV battery cooling and heating by heat pipes, Appl. Therm. Eng. 88 (2015) 54–60.
[18] V. Vishwakarma, C. Waghela, Z. Wei, R. Prasher, S.C. Nagpure, J. Li, et al., Heat transfer enhancement in a lithium-ion cell through improved material-level thermal transport, J. Power Sources 300 (2015) 123–131.
[19] L. Saw, Y. Ye, A. Tay, Feasibility study of Boron Nitride coating on Lithium-ion battery casing, Appl. Therm. Eng. 73 (2014) 154–161.
[20] G. Jiang, J. Huang, Y. Fu, M. Cao, M. Liu, Thermal optimization of composite phase change material/expanded graphite for Li-ion battery thermal management, Appl. Therm. Eng. 108 (2016) 1119–1125.
[21] F. Samimi, A. Babapoor, M. Azizi, G. Karimi, Thermal management analysis of a Li-ion battery cell using phase change material loaded with carbon fibers, Energy. 96 (2016) 355–371.
[22] S. Wilke, B. Schweitzer, S. Khateeb, S. Al-Hallaj, Preventing thermal runaway propagation in lithium ion battery packs using a phase change composite material: an experimental study, J. Power Sources 340 (2017) 51–59.
[23] R. Zhao, J. Gu, J. Liu, Optimization of a phase change material based internal cooling system for cylindrical Li-ion battery pack and a hybrid cooling design, Energy 135 (2017) 811–822.
[24] W. Li, Z. Qu, Y. He, Y. Tao, Experimental study of a passive thermal management system for high-powered lithium ion batteries using porous metal foam saturated with phase change materials, J. Power Sources 255 (2014) 9–15, https://doi.org/10.1016/j.jpowsour.2014.01.006.
[25] L.H. Saw, Y. Ye, M.C. Yew, W.T. Chong, M.K. Yew, T.C. Ng, Computational fluid dynamics simulation on open cell aluminium foams for Li-ion battery cooling system, Appl. Energy 204 (2017) 1489–1499.
[26] N. Javani, I. Dincer, G. Naterer, B. Yilbas, Heat transfer and thermal management with PCMs in a Li-ion battery cell for electric vehicles, Int. J. Heat Mass Transf. 72 (2014) 690–703.
[27] D.W. Hahn, M.N. Özişik, Heat Conduction, 2012.
[28] A.S. Dorfman, Conjugate Problems in Convective Heat Transfer, CRC Press, Boca Raton, 2010.
[29] K. Shah, A. Jain, An iterative, analytical method for solving conjugate heat transfer problems, Int. J. Heat Mass Transf. 90 (2015) 1232–1240.
[30] J. Caldwell, Y. Kwan, On the perturbation method for the Stefan problem with time-dependent boundary conditions, Int. J. Heat Mass Transf. 46 (2003) 1497–1501.
[31] N. Sadoun, E.-K. Si-Ahmed, P. Colinet, On the refined integral method for the one-phase Stefan problem with time-dependent boundary conditions, Appl. Math. Model. 30 (2006) 531–544.
[32] G.E. Myers, Analytical Methods in Conduction Heat Transfer, AMCHT Publ, Madison, WI, 1998.
[33] D. Anthony, D. Sarkar, A. Jain, Non-invasive, transient determination of the core temperature of a heat-generating solid body, Sci. Rep. 6 (2016).
[34] S. Drake, M. Martin, D. Wetz, J. Ostanek, S. Miller, J. Heinzel, et al., Heat generation rate measurement in a Li-ion cell at large C-rates through temperature and heat flux measurements, J. Power Sources 285 (2015) 266–273.
[35] D. Anthony, D. Wong, D. Wetz, A. Jain, Non-invasive measurement of internal temperature of a cylindrical Li-ion cell during high-rate discharge, Int. J. Heat Mass Transf. 111 (2017) 223–231.
[36] Z. Ling, F. Wang, X. Fang, X. Gao, Z. Zhang, A hybrid thermal management system for lithium ion batteries combining phase change materials with forced-air cooling, Appl. Energy 148 (2015) 403–409.